

Ab Initio Study of the $\text{AlX}_3 \cdots 2\text{H}_2\text{O}$ ($\text{X} = \text{F}, \text{Cl}$) and $\text{AlF}_3 \cdots 3\text{H}_2\text{O}$ Complexes

M. Krossner, G. Scholz,* and R. Stösser

Humboldt University of Berlin, Institute of Chemistry, Institute of Physical and Theoretical Chemistry, Hessische Strasse 1-2, D-10115 Berlin, Germany

Received: August 16, 1996; In Final Form: November 6, 1996[⊗]

The structures, binding energies, and harmonic vibrational frequencies of $\text{AlX}_3 \cdots 2\text{H}_2\text{O}$ ($\text{X} = \text{F}, \text{Cl}$) complexes have been explored for the first time at the HF, DFT, and MP2 levels using the 6-31G*, 6-31+G*, and the 6-311G** basis sets. The optimizations were performed without symmetry restrictions or other structural limitations. All complexes investigated were found to be energetically stable, regardless of the computational method used. The calculations showed that the DFT(B3LYP)/6-31+G* method is suitable for the prediction of both binding energies and vibrational frequencies for these types of complexes. This makes possible qualitatively accurate calculations at a relatively low computational expense of even larger, comparable complexes. The $\text{AlF}_3 \cdots 3\text{H}_2\text{O}$ complex was therefore investigated only at this level, yielding the basis for the molecular interpretation of the first steps of the macroscopically investigated hydration process of AlF_3 . A comparison of the binding energies of complexes containing an increasing number of water molecules has been performed. Furthermore, the vibrational frequencies of all complexes have been predicted.

1. Introduction

The physical and chemical properties of aluminum halides and their hydrates are of interest in science as well as in industry.¹ The thermal behavior of the hydrates offers a complexity of processes that have not previously been understood either in macroscopic detail or at a molecular level. Not only physical but also chemical processes govern the thermal phase transitions of aluminum fluoride trihydrates.² They arise from locally alternating dehydration and hydration reactions superimposed on crystalline to amorphous to crystalline transitions determined by the partial pressures of H_2O and HF.^{2a,b} Therefore, the composition of the gaseous phase in the interaction with the solid and with its surface is of importance for the understanding of the processes mentioned above.

Although direct experimental evidence of oxygen-bridged vapor-phase complexes between $\text{AlF}_3(\text{AlCl}_3)$ and H_2O or OH^- is still not available, the existence of such adducts can be predicted based on results of quantum chemical ab initio calculations.^{3,4} $\text{AlF}_3(\text{AlCl}_3) \cdots \text{OH}^-$ or $\text{AlF}_3(\text{AlCl}_3) \cdots \text{H}_2\text{O}$ were found to be energetically stable complexes.³ Owing to the high vapor pressure of solid AlCl_3 and its strong hygroscopic properties, the formation of H_2O adducts should be favored even at ambient temperatures. Moreover, the complex $\text{AlCl}_3 \cdots 2\text{H}_2\text{O}$, which will be discussed among others in this paper, has the same molecular mass as the spectroscopically detected complex $\text{AlCl}_3 \cdots \text{HCl}$.⁵ Therefore, in principle the existence of the $\text{AlCl}_3 \cdots 2\text{H}_2\text{O}$ complex should be taken into account in the mass spectroscopic analysis. Two main aspects drive our interest in gaseous oxygen-bridged water-containing complexes of AlF_3 and AlCl_3 : (i) the description of molecules coexisting in the gaseous phase during thermally induced processes of aluminum halides and (ii) to obtain a deeper understanding of the hydration/dehydration processes and transport properties (e.g., sublimation) of solid aluminum fluorides and chlorides.

It is well-known that solid AlCl_3 reacts immediately with traces of water if, for example, moisture in the air is accessible. As a consequence, the structure of crystalline AlCl_3 will be reorganized in the presence of water until the stable $\text{AlCl}_3 \cdots$

$6\text{H}_2\text{O}$ is formed. The tendency of crystalline $\alpha\text{-AlF}_3$ to undergo hydration processes is remarkably lower. However, the much more active amorphous AlF_3 , obtained, for example, by chemical vapor deposition, exhibits a strong tendency to hydration,⁶ which was proven by FTIR microscopic measurements. It could be shown that vapor-deposited amorphous AlF_3 immediately yields the FTIR spectral pattern of $\alpha\text{-AlF}_3 \cdots 3\text{H}_2\text{O}$ ⁶ when exposed to water.

Therefore, this paper can be regarded as an attempt at the stepwise modeling of the processes of hydration of aluminum fluoride molecules in the gaseous phase and at surfaces of solids. It is our intention to model the first steps of the hydration of AlF_3 and AlCl_3 at a molecular level. Quantum chemical ab initio calculations have been performed for complexes of AlF_3 and AlCl_3 with two or three water molecules, respectively. For this purpose, the results of HF, MP2, and DFT calculations performed using three extended basis sets will be presented and discussed. The capability of DFT calculations in combination with extended basis sets was tested.

2. Methods

Hartree–Fock (HF), Møller–Plesset second-order (MP2), and the density functional-HF hybrid method (DFT-B3LYP) have been used to determine equilibrium structures, binding energies, and harmonic vibrational frequencies of the complexes mentioned in the title. Three different basis sets were adopted: (i) 6-31G*, split valence basis set plus polarization functions on Al, F, O, and Cl;⁷ (ii) 6-31+G*, split valence plus polarization functions and diffuse sp functions on Al, F, O, and Cl;⁸ (iii) 6-311G**, split valence basis set plus polarization functions on all atoms.⁹ Basis set superposition errors (BSSE) have been estimated using the Boys–Bernardi method.¹⁰ The DFT calculations were made adopting Becke's three-parameter hybrid functional (B3LYP),¹¹ which includes a mixture of HF-exchange with DFT exchange-correlation.

The frequencies of harmonic vibrations were calculated for the optimized structures. According to the observation that the harmonic frequencies are systematically larger than observed frequencies, the theoretically predicted frequencies were scaled.

[⊗] Abstract published in *Advance ACS Abstracts*, January 1, 1997.

TABLE 1: Total Energies [au] of the Equilibrium Structures of the $\text{AlX}_3 \cdots 2\text{H}_2\text{O}$ ($\text{X} = \text{F}, \text{Cl}$) Complexes

complex	6-31G*	6-31+G*	6-311G**
HF Optimization			
$\text{AlF}_3 \cdots 2\text{H}_2\text{O}$	-692.554958	-692.581715	-692.720683
$\text{AlCl}_3 \cdots 2\text{H}_2\text{O}$	-1772.673211	-1772.681659	-1772.834763
DFT Optimization			
$\text{AlF}_3 \cdots 2\text{H}_2\text{O}$	-695.082236	-695.128739	-695.271759
$\text{AlCl}_3 \cdots 2\text{H}_2\text{O}$	-1776.135673	-1776.151090	-1776.314575
MP2 Optimization			
$\text{AlF}_3 \cdots 2\text{H}_2\text{O}$	-693.535292	-693.592650	-694.056543
$\text{AlCl}_3 \cdots 2\text{H}_2\text{O}$	-1773.534575	-1773.563137	-1774.044190

TABLE 2: Selected Bond Lengths [pm] and Angles [deg] of the Optimized Structures^a

	$\text{AlF}_3 \cdots 2\text{H}_2\text{O}$			$\text{AlCl}_3 \cdots 2\text{H}_2\text{O}$		
	HF	DFT	MP2	HF	DFT	MP2
$r_{(\text{Al-F1})}$	167	170	169	214	216	213
$r_{(\text{Al-F2})}$	165	167	167	212	213	211
$r_{(\text{Al-F3})}$	165	167	166	211	212	210
$r_{(\text{O1-H1})}$	95	97	96	95	97	97
$r_{(\text{O1-H2})}$	97	101	100	97	101	101
$\angle_{(\text{H1-O1-H2})}$	110	110	109	110	110	110
$r_{(\text{O2-H3})}$	95	98	97	95	97	97
$r_{(\text{O2-H4})}$	95	97	96	95	97	97
$\angle_{(\text{H1O2-H4})}$	108	107	107	107	106	105
$r_{(\text{Al-O1})}$	191	191	192	191	191	192
$r_{(\text{O2-H2})}$	173	159	165	172	158	161
$r_{(\text{F1-H3})}$	202	182	192	295	255	279

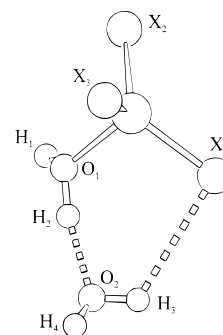
^a Average values of the three basis sets used. The deviations between the optimized structure parameters and the corresponding average values are not larger than ± 2 pm (for distances) and $\pm 1^\circ$ (for angles).

To scale the frequencies, we first evaluated the average of the experimentally available frequencies of the H_2O , AlF_3 , and AlCl_3 molecules, respectively. For each level of theory we then determined the corresponding scaling factor, which makes the average value of the calculated frequencies match the experimental value. The scaling factor obtained for the water molecule differs somewhat from the scaling factors obtained for the AlF_3 and AlCl_3 molecules. Therefore, we used two scaling factors to predict the frequencies of the calculated complexes: one for the H_2O subunit and the average of the AlF_3 and AlCl_3 factors for the AlX_3 subunit. The average value of the scaling factors of H_2O and AlX_3 was taken for the prediction of intermolecular frequencies. This crude scaling procedure accounts for both systematic errors of the calculated harmonic force constants and the neglected anharmonicity effects. All calculations were carried out with the GAUSSIAN92¹² and GAUSSIAN94¹³ programs on IBM RS6000 and HP9000/735 workstations as well as on a CRAY YMP 4D/464 computer.

3. $\text{AlX}_3 \cdots 2\text{H}_2\text{O}$ ($\text{X}=\text{F},\text{Cl}$) Complexes

Optimized Structures. The structures of the complexes were all optimized without symmetry restrictions. Table 1 summarizes the total energies of the optimized complexes. The different basis sets do not result in significant geometrical differences at a particular level of theory. Table 2 therefore collects the average values of selected bond lengths and angles obtained at the HF, DFT, and MP2 levels for the $\text{AlX}_3 \cdots 2\text{H}_2\text{O}$ ($\text{X} = \text{F}, \text{Cl}$) clusters. Figure 1 shows the structure and the labeling of the atoms (no further minima could be located at the potential energy surfaces).

The calculated intramolecular bond lengths and angles are quite similar at all three levels. Only the $\text{O}_1\text{—H}_2$ bond becomes somewhat longer upon including electron correlation (HF gives 97 pm, DFT gives 101 pm, and MP2 gives 100/101 pm for the

**Figure 1.** Structure and labeling of the atoms of the complexes $\text{AlX}_3 \cdots 2\text{H}_2\text{O}$ ($\text{X} = \text{Cl}, \text{F}$).**TABLE 3: Binding Energies, ΔE_B , Basis Set Superposition Errors, BSSE, and Corrections due to Zero-Point Vibrational Energies ZPVE in kJ/mol of the $\text{AlX}_3 \cdots 2\text{H}_2\text{O}$ Complexes^a**

	$\text{AlF}_3 \cdots 2\text{H}_2\text{O}$			$\text{AlCl}_3 \cdots 2\text{H}_2\text{O}$		
	6-31G*	6-31+G*	6-311G**	6-31G*	6-31+G*	6-311G**
HF						
ΔE_B	-217.8	-198.8	-221.4	-198.6	-179.0	-194.0
BSSE	33.2	16.0	30.5	25.7	18.3	25.6
ZPVE	24.2	22.8	23.0	21.4	21.0	23.7
ΣE^b	-160.4	-160.0	-167.8	-151.4	-139.6	-144.6
$\Sigma E/2^c$	-80.2	-80.0	-83.9	-75.7	-69.8	-72.3
DFT						
ΔE_B	-247.0	-203.8	-243.2	-221.8	-179.8	-213.0
BSSE	55.3	16.6	52.5	41.9	17.8	41.6
ZPVE	24.5	23.7	23.0	22.0	21.6	20.1
ΣE^b	-167.2	-163.5	-167.6	-157.9	-140.4	-151.2
$\Sigma E/2^c$	-83.6	-81.9	-83.8	-78.9	-70.2	-75.6
MP2						
ΔE_B	-254.8	-226.0	-240.8	-230.2	-210.4	-218.8
BSSE	68.9	42.3	66.0	58.3	55.4	63.0
ZPVE	<i>e</i>	23.9	23.6	<i>e</i>	<i>e</i>	19.6
ΣE^b	-162.2 ^d	-159.8	-151.2	-152.3 ^d	-156.3 ^d	-136.2
$\Sigma E/2^c$	-81.1 ^d	-79.9	-75.6	-76.1 ^d	-78.1 ^d	-68.1

^a Corrections due to zero-point vibrational energy calculated from nonscaled frequencies. ^b $\Sigma E = \Delta E_B + \text{BSSE} + \text{ZPVE}$. ^c $\Sigma E/2$: ΣE per water molecule. ^d Zero-point vibrational energy contribution taken from the 6-311G** value. ^e Not calculated.

$\text{AlF}_3 \cdots 2\text{H}_2\text{O}$ and $\text{AlCl}_3 \cdots 2\text{H}_2\text{O}$ complexes, respectively). The other intramolecular bond lengths become only marginally longer if electron correlation is included.

Although the short intermolecular Al—O_1 distance is calculated to be about 191–192 pm at all computational levels considered here, the other two intermolecular distances ($\text{O}_2\text{—H}_2$ and $\text{X}_1\text{—H}_3$) are strongly dependent on the method used for the calculations. This sensitivity of the H-bond upon including electron correlation is a well-known fact resulting from the missing dispersion energy at the HF level.¹⁴ At the HF level we calculated the largest intermolecular $\text{O}_2\text{—H}_2$ distances: 173 pm for the $\text{AlF}_3 \cdots 2\text{H}_2\text{O}$ and 172 pm for the $\text{AlCl}_3 \cdots 2\text{H}_2\text{O}$ complex, respectively. By inclusion of electron correlation at the MP2 level, these distances shorten to become 165 and 161 pm. At the DFT level we have the strongest interaction and the shortest intermolecular distances: 159 and 158 pm, respectively. For the $\text{X}_1\text{—H}_3$ distance we calculated even larger differences. For the $\text{AlF}_3 \cdots 2\text{H}_2\text{O}$ complex the difference between the HF and the DFT values is 20 pm and for the $\text{AlCl}_3 \cdots 2\text{H}_2\text{O}$ complex 40 pm.

Binding Energies. Table 3 summarizes calculated binding energies ΔE_B for the $\text{AlX}_3 \cdots 2\text{H}_2\text{O}$ complexes. It is defined as the difference between the total energy of the complex and the sum of the total energies of the free molecules AlX_3 and water:

$$\Delta E_B = E_{\text{complex}} - E_{\text{AlX}_3} - 2E_{\text{water}}$$

As expected, the MP2 values are larger than those calculated at the HF level. In absolute terms, the complexes calculated at the MP2 level are about 20–40 kJ/mol more stable than those calculated at the HF level. The smallest differences between HF and MP2 results are obtained using the largest basis set (6-311G**, cf. Table 3).

The interaction calculated at the DFT level with the 6-31G* and 6-311G** basis sets is also about 20–30 kJ/mol larger than that at the HF level, but the absolute values of the binding energy are somewhat smaller than at the MP2 level. For the 6-31+G* basis set, however, the HF and DFT binding energies appear to be quite similar: for $\text{AlF}_3 \cdots 2\text{H}_2\text{O}$, -199 kJ/mol(HF) and -204 kJ/mol (DFT), and for $\text{AlCl}_3 \cdots 2\text{H}_2\text{O}$, -179 kJ/mol(HF) and -180 kJ/mol (DFT). The absolute values of the corresponding MP2 energy were calculated to be almost 30 kJ/mol larger.

The basis set superposition error is calculated to be smallest for the 6-31+G* basis set. This fact was already observed in previous investigations of heterodimer complexes like $\text{AlX}_3 \cdots \text{H}_2\text{O}$.³ At the HF level the BSSE is less than 20 kJ/mol for this basis set, whereas the other two basis sets result in BSSEs of about 30 kJ/mol ($\text{AlF}_3 \cdots 2\text{H}_2\text{O}$) and 26 kJ/mol ($\text{AlCl}_3 \cdots 2\text{H}_2\text{O}$). At the MP2 level these errors increase and we obtain values of up to 70 kJ/mol for the 6-31G* and 6-311G** basis sets, which mean almost 30% of the binding energy. For the 6-31+G* basis set, superposition errors reach less than 20% of the binding energy. At the DFT/6-31+G* level the BSSE amounts to less than 10%, which is comparable with the HF values. For the other two basis sets we predict a BSSE of about 20% of the binding energy. Owing to the relatively small basis set superposition errors, the use of the 6-31+G* can be recommended as particularly favorable.

Zero-point vibrational energies for all complexes were calculated to be approximately 20–25 kJ/mol.

Considering all energies contributions, we obtain, dependent on the method and basis set used, binding energies per water molecule for the $\text{AlF}_3 \cdots 2\text{H}_2\text{O}$ complex between -78 and -84 kJ/mol. The corresponding value for the $\text{AlCl}_3 \cdots 2\text{H}_2\text{O}$ complex is calculated between -68 and -79 kJ/mol.

Previous calculations of heterodimer complexes predicted binding energies of about -122 to -130 kJ/mol for the $\text{AlF}_3 \cdots \text{H}_2\text{O}$ complex and about -105 to -113 kJ/mol for the $\text{AlCl}_3 \cdots \text{H}_2\text{O}$ complex.³ Considering the zero-point vibrational energy correction, these values are predicted to be reduced by about 10 kJ/mol. However, as expected, these estimated values are still significantly larger than the binding energies per water molecule of the corresponding $\text{AlX}_3 \cdots 2\text{H}_2\text{O}$ complexes.

Harmonic Vibrational Frequencies. The calculated harmonic frequencies are summarized in Table 4. In general, the most reliable frequencies are expected for the largest basis set (6-311G**) at the MP2 level. The calculations at this level are very computer time expensive. In order to determine the reliability of the vibrational analysis of the other theoretical levels, we also calculated the vibrational frequencies at these levels. These calculations will result in frequencies with more or less significant differences to the MP2/6-311G** values. It is especially interesting to see how well the DFT frequencies agree with the MP2 results. The frequency at the HF level for the sensitive $\text{O}_1\text{—H}_2$ bond (red-shifted by the influence of the $\text{O}_2 \cdots \text{H}_2$ hydrogen bond) is expected to be calculated at too high wavenumbers. The calculated frequencies will be separately discussed for $\text{AlF}_3 \cdots 2\text{H}_2\text{O}$ and $\text{AlCl}_3 \cdots 2\text{H}_2\text{O}$.

All methods predict quite similar frequencies for the “free” OH bonds not involved in hydrogen bonds of $\text{AlF}_3 \cdots 2\text{H}_2\text{O}$. The

basis set dependence is also only minor. Furthermore, the vibrational frequencies of the AlF_3 subunit are also quite insensitive to the method chosen. The differences between the frequencies calculated at different levels do not exceed 10 cm^{-1} . Moreover, there are no great shifts in comparison to the vibrational frequencies of the free AlF_3 molecule, which are experimentally determined at 263 , 297 , 655 ± 5 , and 935 cm^{-1} .^{16,17b} However, it should be mentioned that previous ab initio calculations performed for the AlF_3 and AlCl_3 molecules are not free from disagreements with experimentally assigned frequencies.¹⁷

Obviously, the characteristic mode of this complex appears to be the strongly red-shifted ν_{OH} mode of the $\text{O}_1\text{—H}_2$ bond. At this frequency also the most intense band in the IR spectrum results. This large red shift reflects the influence of the $\text{H}_2 \cdots \text{O}_2$ hydrogen bond, resulting in a remarkably elongated $\text{O}_1\text{—H}_2$ bond ($97 \rightarrow 101 \text{ pm}$). For this vibration mode the differences between the applied calculation methods are the largest. First, we find significant differences between the predictions of the HF and MP2 methods. The red shift of the ν_{OH_2} stretching mode is much larger when electron correlation is included. At the MP2 level this frequency is calculated at 2895 cm^{-1} and at the HF level at 3230 cm^{-1} . The DFT method, on the other hand, predicts larger shifts of the OH stretching frequency than the MP2 method. The DFT frequency is calculated to be 2794 cm^{-1} , i.e., 100 cm^{-1} below the MP2 value.

In this connection, one interesting fact should be noticed: the DFT/6-31+G* method virtually reproduces the MP2/6-311G** value of the characteristic ν_{OH_2} frequency. Obviously, we have a favorable case of error compensation. The DFT/6-31+G* value of 2908 cm^{-1} is only 13 cm^{-1} lower than the MP2/6-311G** value. Additionally, the other ν_{OH} frequencies are qualitatively reproduced: DFT/6-31+G* gives 3726 , 3681 , and 3506 cm^{-1} and MP2/6-311G** gives 3706 , 3673 , and 3505 cm^{-1} . The rather small red shift of about 200 cm^{-1} for the third value for each level of theory has its origin in the fact that there is also a $\text{H} \cdots \text{F}$ hydrogen bond that causes a slight elongation of the corresponding $\text{O}_2\text{—H}_3$ bond ($97 \rightarrow 98 \text{ pm}$; see table 2).

The HOH deformation modes are calculated to be about 80 cm^{-1} higher than at the MP2/6-311G** level. However, these frequencies are not the characteristic ones in a first attempt to interpret the spectrum. Their intensity is relatively small, and the shift in comparison to the frequency of free water molecules (1595 cm^{-1} ¹⁴) is not substantial. Furthermore, the DFT/6-31+G* frequencies of the AlF_3 unit are in good agreement with the MP2/6-311G** results: 893 vs 886 cm^{-1} , 832 vs 825 cm^{-1} , 650 vs 641 cm^{-1} , 300 vs 293 cm^{-1} , 253 vs 250 cm^{-1} , and 245 vs 240 cm^{-1} . Hence, the DFT/6-31+G* method is obviously suitable for frequency calculations resulting in MP2/6-311G** quality even for the sensitive characteristic ν_{OH_2} mode. The computational costs are smaller by far. Therefore, besides the already observed small BSSE, we get further arguments for the adoption of the DFT/B3LYP method in combination with a 6-31+G* basis set.

For the $\text{AlCl}_3 \cdots 2\text{H}_2\text{O}$ complex one of the most interesting questions is whether the error compensation of the DFT/6-31+G* method, which was observed for $\text{AlF}_3 \cdots 2\text{H}_2\text{O}$, can be reproduced for other comparable complexes such as this one. The MP2/6-311G** value of the characteristic ν_{OH_2} mode is calculated to be at 2934 cm^{-1} , and the HF value is predicted at far too high wavenumbers: 3148 cm^{-1} . The DFT/6-311G** method again yields too large a red shift. The ν_{OH_2} frequency is calculated to be 121 cm^{-1} lower than the corresponding MP2 value. Also, in this case calculations at the DFT/6-31+G* level

TABLE 4: Selected Harmonic Vibrational Frequencies for the Calculated $\text{AlX}_3 \cdots 2\text{H}_2\text{O}$ ($\text{X} = \text{F}, \text{Cl}$) Complexes [cm^{-1}]^a

	$\text{AlF}_3 \cdots 2\text{H}_2\text{O}$						$\text{AlCl}_3 \cdots 2\text{H}_2\text{O}$							
	HF		DFT		MP2		HF		DFT		MP2			
	6-31G*	6-31+G*	6-31G**	6-31+G**	6-31G*	6-31+G*	6-31G**	6-31+G**	6-31G*	6-31+G*	6-31G**	6-31+G**		
ν_{OH}	3683	3728	3724	3711	3726	3718	3700	3706	3728	3712	3713	3721	3713	3695
ν_{OH}	3625	3656	3675	3688	3681	3700	3681	3673	3659	3678	3696	3666	3696	3661
ν_{OH}	3550	3598	3593	3436	3506	3468	3506	3505	3629	3569	3590	3569	3590	3603
ν_{OH2}	3196	3279	3230	3276	2908	2794	2908	2895	3199	2783	2907	2907	2813	2934
δ_{HOH}	1629	1647	1582	1682	1667	1599	1667	1582	1642	1673	1606	1665	1600	1569
δ_{HOH}	1615	1620	1557	1653	1635	1571	1635	1555	1630	1644	1570	1633	1566	1553
ν_{AlX}	907	886	890	920	893	902	893	886	541	550	541	567	563	564
ν_{AlX}	847	830	831	849	832	837	832	816	520	512	512	520	532	542
ν_{AlX}	665	660	656	662	650	650	650	641	364	359	363	365	366	372
δ_{XAlX}	301	294	294	311	300	300	300	293	192	193	193	197	197	197
δ_{XAlX}	256	248	244	268	253	257	253	250	165	164	164	172	160	164
δ_{XAlX}	245	237	230	252	245	242	245	244	124	124	126	127	120	126
δ_{XAlX}	972	945	924	1189	1114	1119	1114	1085	921	945	945	1089	1073	1030
interm	689	680	676	765	744	741	744	725	731	725	725	772	776	765
interm	568	528	529	735	655	669	655	619	490	605	516	539	511	510
interm	474	474	483	514	503	514	503	507	419	502	472	497	480	465
interm	406	378	359	503	452	435	441	441	350	441	462	415	381	412
interm	329	326	331	386	380	381	380	362	283	378	412	355	321	330
interm	280	274	267	339	328	322	328	291	265	312	348	319	264	298
interm	234	192	204	329	287	287	287	238	182	287	247	226	198	190
interm	170	159	164	212	170	196	170	175	157	184	192	183	172	173
interm	149	147	140	166	144	158	144	154	111	155	113	115	110	112
interm	142	126	135	158	154	150	154	149	71	154	83	107	90	70
interm	34	34	34	42	41	43	41	38	17	38	42	19	14	30

^a Adopted scaling factors. 6-31G* HF: 0.8878 (H_2O)/0.9233 (AlX_3)/(0.8878 + 0.9233)/2 = 0.9056 (intermolecular). 6-31G* DFT: 0.9782/0.9709/0.9745. 6-31G* MP2: See footnote b. 6-31+G* HF: 0.8973/0.9352/0.9162. 6-31+G* DFT: 0.9762/0.9918/0.9840. 6-31+G* MP2: 0.9704/0.9618/0.9661. 6-311G** HF: 0.8846/0.9296/0.9071. 6-311G** DFT: 0.9605/0.9824/0.9714. 6-311G** MP2: 0.9352/0.9471/0.9411. ^b Not calculated.

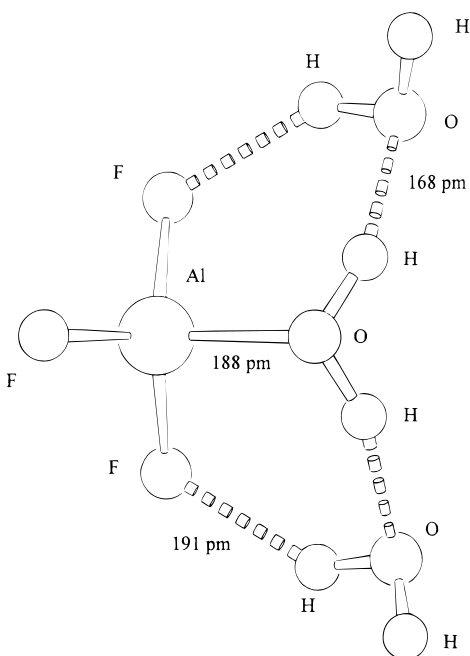


Figure 2. Equilibrium structure of the complex $\text{AlF}_3 \cdots 3\text{H}_2\text{O}$ calculated at the DFT/6-31+G* level.

result in the much better value of 2907 cm^{-1} , i.e., the difference amounts to only 24 cm^{-1} . Differences for the other ν_{OH} frequencies are also not larger than 35 cm^{-1} . The HOH deformation modes again show a larger deviation, whereas the frequencies of the AlCl_3 subunit are in good agreement compared with the MP2 results. The shifts compared with the experimental frequencies of the free AlCl_3 molecule are, as for the $\text{AlF}_3 \cdots 2\text{H}_2\text{O}$ complex, not particularly large. IR active frequencies in AlCl_3 are experimentally determined at 616, 371, 214, and 148 cm^{-1} ,^{16,17a} whereas the corresponding frequencies (DFT/6-31+G*) in the complex were calculated to be 567, 365, 197, and 127 cm^{-1} .

The calculated binding energies of the $\text{AlX}_3 \cdots 2\text{H}_2\text{O}$ complexes showed that all methods adopted here result in similar binding energies if all energy contributions (BSSE, ZPVE) were taken into account. For the 6-31+G* basis set we obtained the smallest basis set superposition errors. Furthermore, the vibrational frequency calculations showed that by use of the DFT method, the calculated vibrational frequencies are of MP2/6-311G** quality. Encouraged by these findings the calculations for the $\text{AlF}_3 \cdots 3\text{H}_2\text{O}$ complex were carried out only at the DFT/6-31+G* level. Reliable results at acceptable computational effort are expected.

4. $\text{AlF}_3 \cdots 3\text{H}_2\text{O}$ Complex

Figure 2 shows the optimized structure of the $\text{AlF}_3 \cdots 3\text{H}_2\text{O}$ complex, which is the global minimum at the potential energy surface. (It should be noted that the stable solid phase of aluminum fluoride hydrates has the same chemical composition but exhibits a completely different structure. Further energetically discriminated local minima of the complex could be obtained by rotation of the hydrogen-bonded water molecules leading to C_1 symmetries.) We now have two water molecules hydrogen bonded to the third one. The optimization process results in a structure with C_s symmetry. In Table 5 the binding energies for the $\text{AlF}_3 \cdots (\text{H}_2\text{O})_n$, $n = 1, 2, 3$ complexes are compared. Additionally, the binding energies are averaged among the number of water molecules. The largest binding energy per water molecule is obtained for the smallest complex $\text{AlF}_3 \cdots \text{H}_2\text{O}$: -105.7 kJ/mol . By addition of a second water

TABLE 5: Comparison of the Binding Energies [kJ/mol] of the $\text{AlF}_3 \cdots (\text{H}_2\text{O})_n$ ($n = 1, 2, 3$) Complexes at the DFT/6-31+G* Level

n	$1\text{H}_2\text{O}^a$	$2\text{H}_2\text{O}$	$3\text{H}_2\text{O}$
ΔE_{B}	-126.2	-203.8	-269.0
BSSE	9.2	16.6	23.3
ZPVE	11.3	23.7	36.6
ΣE	-105.7	-163.5	-209.1
ΣE per water	-105.7	-81.9	-69.7

^a See also ref 2.

TABLE 6: Comparison of the Most Important Bond Lengths [pm] of the Complexes $\text{AlF}_3 \cdots n\text{H}_2\text{O}$ ($n = 1, 2, 3$)

	$\text{AlF}_3 \cdots \text{H}_2\text{O}$	$\text{AlF}_3 \cdots 2\text{H}_2\text{O}$	$\text{AlF}_3 \cdots 3\text{H}_2\text{O}$
R (O \cdots H) ^a		162	168
R (F \cdots H) ^a		188	191
R (Al-O)	197	192	188
R (Al-F)	167	167	167
R (Al-F) ^a		170	170

^a Hydrogen bond. ^b Hydrogen-bonded F.

molecule to the complex, the binding energy per water molecule is reduced by about 24 kJ/mol . A third water molecule further reduces the binding energy per water molecule to -70 kJ/mol .

As shown in Figures 1 and 2, the nature of the chemical interaction is quite different for the three water molecules. Therefore, we abandon the crude averaging of the binding energies over all water molecules and consider the specific contributions in more detail. The most energetically favorable interaction is that of the O-Al (Lewis type) bonded first water molecule. As we see from the calculations of the $\text{AlF}_3 \cdots \text{H}_2\text{O}$ complex, this should result in a contribution of about -106 kJ/mol to the binding energy. The second and the third water molecule are each bonded by two (H \cdots O, H \cdots F) hydrogen bonds. The difference between the binding energy of the $\text{AlF}_3 \cdots \text{H}_2\text{O}$ complex and the $\text{AlF}_3 \cdots 2\text{H}_2\text{O}$ complex implies a contribution of about -58 kJ/mol for this type of bonding. Therefore, we can estimate a value of about -222 kJ/mol for the $\text{AlF}_3 \cdots 3\text{H}_2\text{O}$ complex. The calculated value is -210 kJ/mol . That means that in the case of adsorption of a third water molecule the bonding of the others is slightly weakened.

The formation of complexes of AlF_3 with up to three water molecules is energetically favorable compared to pure water complexes. The binding energy calculated for the water dimer at the DFT/6-31+G* level was only -11.7 kJ/mol , considering BSSE and ZPVE. This value justifies the assumption of complex formation of water molecules with AlF_3 and AlCl_3 , since a further stabilization is predicted in the latter case.

In the calculated IR spectrum of $\text{AlF}_3 \cdots 3\text{H}_2\text{O}$ we have two ν_{OH} frequencies of "free" OH bonds: 3732 and 3731^3 (all frequencies of the calculated spectra are scaled using the scaling factors summarized in the caption of Table 4). Furthermore, there are two slightly red-shifted frequencies belonging to the OH bonds influenced by the rather weak H \cdots F hydrogen bond (3532 and 3529 cm^{-1}). The two characteristic vibrational modes of the complex, the strongly red-shifted ν_{OH} frequencies resulting from the hydrogen-bonded OH bonds, are against the most intense bands in the spectrum calculated at 3095 and 3091 cm^{-1} , respectively.

Vibrational modes of the HOH of the three water molecules are calculated at 1688, 1643, and 1636 cm^{-1} . The AlF_3 subunit produces frequencies of 863, 822, 644, 306, 258, and 240 cm^{-1} . Table 6 compares the most important structural parameters of the three complexes. It can be seen that the Al-O bond is slightly shortened if additional water molecules are adsorbed. This can be explained by the appearance of hydrogen bonds

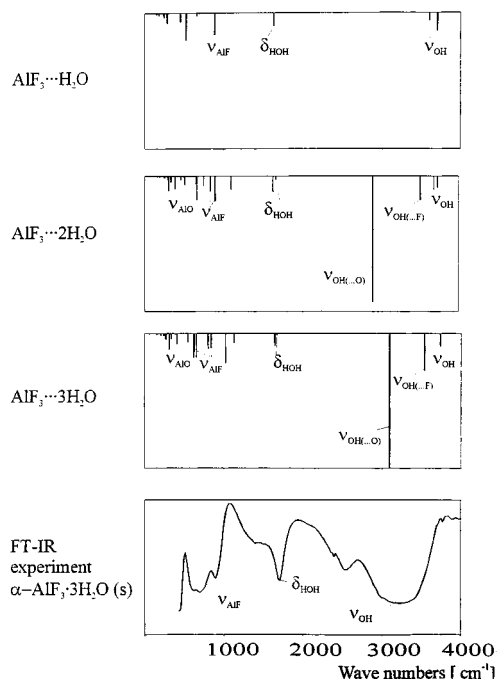


Figure 3. Calculated spectra of the complexes $\text{AlF}_3 \cdot n\text{H}_2\text{O}$ ($n = 1, 2, 3$) and experimental FTIR spectrum of solid $\alpha\text{-AlF}_3 \cdot 3\text{H}_2\text{O}$.⁶

forming a ring structure that involves the Al–O bond. We observe a slight elongation of the length of the hydrogen bonds of the $\text{AlF}_3 \cdot 3\text{H}_2\text{O}$ complex compared with those of the $\text{AlF}_3 \cdot 2\text{H}_2\text{O}$ complex. These small structural changes may be considered the reason for the above-mentioned slight weakening of the bonds. In Figure 3 the calculated vibrational spectra of $\text{AlF}_3 \cdot n\text{H}_2\text{O}$ ($n = 1, 2, 3$) (DFT/B3LYP, 6-31+G* basis set) are shown together with the FTIR spectrum of solid $\alpha\text{-AlF}_3 \cdot 3\text{H}_2\text{O}$.⁶ A good correspondence between the calculated vibrational frequencies of the $\text{AlF}_3 \cdot (\text{H}_2\text{O})_n$ complexes and the experimentally determined IR frequencies of crystalline $\alpha\text{-AlF}_3 \cdot 3\text{H}_2\text{O}$ can be established.

5. Conclusions

No qualitative differences in the binding energies were observed between the different methods as long as all energy contributions were considered. At each level of theory the 6-31+G* basis set yields the smallest basis set superposition errors, which indicates a proper choice of the basis set for this method. Especially at the DFT level the BSSE of only 10% of the binding energy is favorable, since electron correlation can be included without the drawback of large basis set superposition errors. The BSSEs at the MP2 level were calculated to be much larger.

Furthermore, the IR spectra calculated at DFT/6-31+G* level are expected to be quite reliable, and therefore, they can be helpful in the interpretation of measured bands or for predicting IR spectra (e.g., of intermediates of chemical reactions). For larger systems of the type $(\text{AlX}_3)_n \cdot (\text{H}_2\text{O})_m$ qualitatively good frequency calculations become feasible by adopting the DFT/B3LYP method in combination with a 6-31+G* basis set.

HF calculations reveal results of much lower quality for the systems calculated. Although the binding energies are qualitatively well reproduced, the harmonic vibrational frequencies show some unacceptable qualitative errors in comparison to the methods including electron correlation. In particular the lack of a red shift of the characteristic ν_{OH_2} mode upon complex formation must be regarded as a severe disadvantage.

The comparison of the $\text{AlF}_3 \cdot \text{H}_2\text{O}$, $\text{AlF}_3 \cdot 2\text{H}_2\text{O}$, and $\text{AlF}_3 \cdot 3\text{H}_2\text{O}$ complexes shows a reduction of the binding energy per water molecule with increasing number of water molecules. The adsorption energy of the first water molecule interacting with AlF_3 is almost twice as large as for each of the two further adsorbed water molecules.

The existence of $\text{AlX}_3 \cdot 2\text{H}_2\text{O}$ and $\text{AlF}_3 \cdot 3\text{H}_2\text{O}$ complexes is predicted as a result of these calculations if we assume an adequate number of water molecules in the gaseous phase. Considering a comparable amount of AlF_3 and H_2O molecules in the gaseous phase, preferably the $\text{AlF}_3 \cdot \text{H}_2\text{O}$ species should be formed rather than higher adducts. The challenge to the experimentalists is to prove the existence of these complexes directly. The predicted frequencies will furthermore help to assign bands in the corresponding experimental IR spectra. In order to get a deeper insight into the chemistry of the complex formation of AlF_3 and H_2O , it is also essential to investigate complexes including more than one AlF_3 molecule. This will be done in a future study.

Acknowledgment. Financial support from the Deutsche Forschungsgemeinschaft and computer time on the CRAY-YMP of the Konrad-Zuse-Zentrum für Informationstechnik Berlin are gratefully acknowledged. Special thanks go to J. Bartoll for the performance of preliminary calculations as well as to Arne Dummer for technical assistance.

References and Notes

- (1) Fluoride Glasses; Comyns, A. E.; J. Wiley & Sons: Chichester, 1989.
- (2) (a) Menz, D.-H.; Mensing, Ch.; Hönle, W.; v. Schnering, H. G. Z. *Anorg. Allg. Chem.* **1992**, 611, 107. (b) Scholz, G.; Stösser, R.; Sebastian, S.; Kemnitz, E.; Bartoll, J. *J. Phys. Chem. Solids*, submitted.
- (3) Scholz, G.; Stösser, R.; Bartoll, J. *J. Phys. Chem.* **1996**, 100, 6518.
- (4) Ball, D. W. *J. Phys. Chem.* **1995**, 99, 12786.
- (5) Rabeneck, H.; Schäfer, H. Z. *Anorg. Allg. Chem.* **1973**, 395, 69.
- (6) Hoffmann, S. Diploma Thesis, Humboldt-Universität zu Berlin, 1996.
- (7) (a) Hehre, W. J.; Radom, L.; v. R. Schleyer, P.; Pople, J. A. *Ab initio molecular orbital theory*; Wiley: New York, 1986. (b) Hariharan, P. C.; Pople, J. A. *Theor. Chim. Acta* **1973**, 28, 213.
- (8) Clark, T.; Chandrashekar, J.; Spitznagel, G. W.; Schleyer, v. R. P. *J. Comput. Chem.* **1983**, 4, 294.
- (9) (a) Krishnan, R.; Binkley, J. S.; Seeger, R.; Pople, J. A. *J. Chem. Phys.* **1980**, 72, 650. (b) McLean, A. D.; Chandler, G. S. *J. Chem. Phys.* **1980**, 72, 5639.
- (10) Boys, S. F.; Bernardi, F. *Mol. Phys.* **1970**, 19, 553.
- (11) Becke, A. D. *J. Chem. Phys.* **1993**, 98, 5648.
- (12) Frisch, M. J.; Trucks, G. W.; Head-Gordon, M.; Gill, P. M. W.; Wong, M. W.; Foresman, J. B.; Johnson, B. G.; Schlegel, H. B.; Robb, M. A.; Replogle, E. S.; Gomperts, R.; Andres, J. L.; Raghavachari, K.; Binkley, J. S.; Gonzalez, C.; Martin, R. L.; Fox, D. J.; DeFrees, D. J.; Baker, J.; Stewart, J. J. P.; Pople, J. A. *GAUSSIAN 92*, Revision C; Gaussian Inc.: Pittsburgh, PA, 1992.
- (13) Frisch, M. J.; Trucks, G. W.; Schlegel, H. B.; Gill, P. M. W.; Johnson, B. G.; Robb, M. A.; Cheeseman, J. R.; Keith, T.; Petersson, G. A.; Montgomery, J. A.; Raghavachari, K.; Al-Laham, M. A.; Zakrzewski, V. G.; Ortiz, J. V.; Foresman, J. B.; Peng, C. Y.; Ayala, P. Y.; Chen, W.; Wong, M. W.; Andres, J. L.; Replogle, E. S.; Gomperts, R.; Martin, R. L.; Fox, D. J.; Binkley, J. S.; DeFrees, D. J.; Baker, J.; Stewart, J. J. P.; Head-Gordon, M.; Gonzalez, C.; Pople, J. A. *GAUSSIAN 94*, Revision B.3; Gaussian, Inc.: Pittsburgh PA, 1995.
- (14) Krossner, M.; Sauer, J. *J. Phys. Chem.* **1996**, 100, 6199.
- (15) Hargittai, M.; Kolonits, M.; Tremmel, J.; Fourquet, J.-L.; Ferey, G. *Struct. Chem.* **1989**, 1, 75.
- (16) Nakamoto, K. *Infrared and Raman Spectra of Inorganic and Coordination Compounds*; John Wiley & Sons: New York, 1978; Vol. 3.
- (17) (a) Ystenes, B. K.; Ystenes, M.; Scholz, G. *Spectrochim. Acta, Part A* **1995**, 51, 2481. (b) Scholz, G.; Schöffel, K.; Jensen, V. A.; Bache, O.; Ystenes, M. *Chem. Phys. Lett.* **1994**, 230, 196.
- (18) Kaldor, A.; Porter, R. F. *J. Am. Chem. Soc.* **1971**, 93, 2140.
- (19) Curtiss, L. A.; Scholz, G. *Chem. Phys. Lett.* **1993**, 205, 550.
- (20) Klæboe, P.; Rytter, E.; Sjøgren, C. E. *J. Mol. Struct.* **1984**, 113, 943.